



Numerical Methods in Civil Engineering

Journal Homepage: <https://nmce.kntu.ac.ir/>



Performance assessment of seismically-designed steel moment-resisting structures against numerically-simulated blast wave propagation

Hamid Ghanbari^{*}, Eysa Salajegheh^{**} and Javad Salajegheh^{***}

ARTICLE INFO

RESEARCH PAPER

Article history:

Received:

April 2022.

Revised:

July 2022.

Accepted:

July 2022.

Keywords:

Numerical Simulation,

Blast Impact Wave,

Computational Fluid

Dynamics,

Nonlinear time-history

Response

Abstract:

The main goal of this research is the performance evaluation of the sampled moment-resisting steel structure against 3D simulated blast loading. In the first stage of the present research, the numerically simulated blast wave is verified by comparing with the relevant renowned numerical and experimental previous researches. In the second stage, the sensitivity of blast-induced pressure to the finite element mesh size and the surrounding air cube dimensions are investigated considering the 3D one-story building block with real dimensions based on Computational Fluid Dynamics (CFD) using AUTODYN hydrocode. The innovation of this stage is to present the optimum mesh size and air cube dimensions for the numerical results compared with the relevant empirical relationships toward the realistic simulation of blast-induced pressure on structures. Finally, in the last stage, the performances of two seismically-designed buildings with 1 and 10 stories against the achieved numerical blast-induced pressure time histories and the empirical formulations, based on the UFC 3-340-02 guideline, are studied. To assess the structural performance, the sampled buildings are modeled using the finite element tool OpenSEES. Performance assessment of sampled structures reveals that empirical formulation of blast loading will lead to underestimation of structural response, especially for the lower scaled distance scenarios.

1. Introduction

Nowadays, due to the increase of terrorist attacks to the critical structures, the performance assessment of buildings against blast wave is of great importance towards achieving the passive defense goals [1]. Generally, three methods are used to assess the explosion effects on structures, which are empirical, analytical, and numerical simulation methods. Practical methods were developed based on experimental results, which suffer from the limited number of available experiments, high cost, and difficulty of tests for the explosion phenomena. The analytical method was developed based on a simplified representation of physical events through simple analytical models

Therefore, the analytical approach can present the solution for the problems with simple geometry and boundary conditions. On the other hand, numerical methods have the capability of involving more effective parameters. Consequently, more accurate results are expected. Numerical methods gain the attention of various researches in recent years, owing to the enhancement of computational capabilities of computers and developing more precise numerical methods. These methods were developed based on numerical solving of the governing differential equations, while they are in progress towards achieving more accuracy and less computational time. Considering numerically-simulated blast waves in performance assessment of structures against explosion will lead to more realistic results. To achieve this goal, optimum mesh size and air cube dimension are critical parameters.

Extensive researches have been conducted to assess the behavior of structures against the direct and indirect effects of blast loading. The one by Krauthammer et al. [2], entitled simulation of blast loading on reinforced concrete structures,

^{*} Corresponding Author: PhD Candidate, Shahid Bahonar University of Kerman, Iran. Email: hamid.ghanbari@eng.uk.ac.ir

^{**} Professor of civil engineering department, Shahid Bahonar University of Kerman, Iran. Email: eysasala@uk.ac.ir

^{***} Professor of civil engineering department, Shahid Bahonar University of Kerman, Iran. Email: jsalajegheh@uk.ac.ir

<https://doi.org/10.52547/NMCE.2022.420>

concluded that selection of fine mesh size would affect deformation and stress results, considerably. Luccioni et al. [3] studied the effects of propagation of blast wave in air and reflection effect on a finite air volume of $5 \times 10 \times 5$ meters using Hydrocodes (without structure modeling). They concluded that the selection of larger mesh sizes could be made to achieve the rational results towards a comparison of blast-induced loads. Even the mesh size selection greater than 50cm can result in a fair prediction of blast-induced displacement. Furthermore, regarding the effects of mesh size on numerical simulation of blast wave by AUTODYN 2D, the study conducted by Chapman et al. [4] can be mentioned. They proposed a correction factor which tunes the simulation data when the large mesh size is used. Dharaneepathy et al. [5] assessed the effects of blast distance on the structures. The distance is presented as the design scenario for tall buildings. Since the distance triggers the most effects of blast impact on the buildings.

Ghanbari and Salajegheh [6] simulated the 3D blast wave propagation on the building block. Through their study, the effects of meshing size and comparison of empirical formulation and numerical simulation are conducted. Through another research by Ghanbari and Salajegheh [7], the performance assessment of seismically-designed sampled steel moment-resisting frames is achieved against a simulated blast wave. Wenjiao et al. [8] simulated the concrete cracked slabs under blast loading using the LS-DYNA. They concluded that a finite element method is a suitable approach to the prediction of the dynamic behavior of cracked concrete slabs. Moreover, the effect of crack orientation, width, and depth on the response of structure against blast loading was studied. Tavakoli et al. [9] studied the effect of modeling the post-buckling on the best location of belt trusses for tall buildings against blast loading. They concluded that, for detonation distance less than 5 meters, the effect of including the post-buckling behavior is more evident, towards achieving the best location of belt trusses for tall buildings. According to the mentioned researches, performance assessment of 3-dimensional multi-story structures against numerically-simulated blast wave effects has not been conducted.

One of the fundamental properties of the numerical methods, towards the simulation of blast wave propagation phenomena, is the optimum mesh sizes. Due to the limitations of computational capacities, using a very fine mesh size results in substantial computational effort. Therefore, the optimum selection of the mesh size towards the simulation of the blast wave and the relevant interaction with structure, in view of achieving more accurate results while consuming less computational time, is a very influential parameter. To achieve this goal in 3D simulation, usually, the 10^6 - 10^7 elements are applied. As an illustration, simulation of 25×10^{-3} second duration of blast loading on

structure, conducted by Bevins [10] with 38 million meshes required 160 hours using 23 processors of supercomputer Compaq sc45. The element number and the mesh size are dependent on the blast scenario. The mesh size, which is sufficiently fine for a high scaled-distance situation, may be considered to be so coarse for a short scaled-distance one

The simulation of blast waves using the numerical method is done towards a variety of applications. Through the mentioned studies, the main goal was to improve the numerical methods in comparison with the experimental results. As the results of the achieved improvement, recently, the numerical simulation got to the point of being a confident substitute for high-risk, high-cost experiments. Towards achieving this target, Sugiyama et al. [11] presented a fast numerical simulation method. This method was proposed based on the state equation JWL and the results of the study by Flood [12]. They tried to improve the simulation of the blast wave propagation using the numerical simulation through the free domain. Although the mentioned studies recommended some rules to select suitable mesh sizes, further researches are needed owing to the unknown effects of mesh size on the blast parameters. Besides, the dependency of the appropriate mesh size on the scaled and standoff distance is the potential field of research. To the best of the authors' knowledge, the previous studies to consider the blast effects on structures were mostly assessed 2D models, empirical formulation of blast loading are considered. On the other hand, the previous studies which applied numerical method, the limited dimensions of air cubes are used. Furthermore, the primary concern of the previous studies was assessing the wave propagation problem rather than the interaction of propagated waves with the structures (i.e., reflection, refraction, and suction).

In the present research, the effects of mesh size and dimension of air cube, flowing surrounding the structure, on the simulated blast shock wave affected the building structures, are assessed. The effects of the mentioned parameters are measured by the calculated blast wave time-history. Furthermore, the suitable mesh size is proposed according to the scaled distance and standoff distance. The achieved numerical results for different scaled distance and boundary conditions are compared with the relevant empirical formulations and experimental data. Consequently, practical recommendations regarding the selection of suitable mesh size and air cube dimensions are proposed based on the scaled and standoff distances of the blast scenario. Finally, two seismically-designed sampled structures of one and ten stories are analyzed against achieved numerical blast wave. The structural performance against the blast wave effects is assessed against experiential and numerical blast wave. Based on this goal, the structural analyses are performed against the numerical blast wave and experiential formulation of the blast wave using UFC 3-320-

02 graphs. The 3D model of the structure is implemented using OPENSEES. The non-linear dynamic analysis results are calculated towards performance assessment based on FEMA-356 criteria, for which the maximum inter-story drift ratio (MIDR) is the measure of structural performance.

2. Materials and Methods

2.1 Blast load definition

The explosion phenomena result in sudden energy release in the forms of light, air pressure, sound, and heat. The resultant increase in the air pressure is propagated in the way of blast impact wave, which affects the structures [13-16]. In figure (1), the impact of blast wave time history is shown in the free field. The sudden increase in pressure is called the positive pressure phase. In the positive step, the pressure is increased to the maximum value (P_{so}) in the arrival time (t_a), and then it is reduced to the ambient pressure in t_0 .

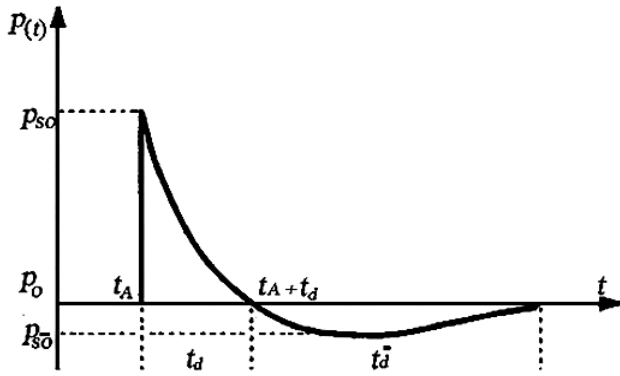


Fig. 1: Blast-induced pressure-time history curve [15]

2.2 Blast impact wave parameters

Blast impact wave parameters were attained through examinations conducted between 1950 and 1960. Usually, a method called scaled distance is used to measure these parameters. The blast scaling method, first put into the formula by Hopkinson in 1919 and then enhanced by Cranz in 1926, is now entitled as Hopkinson-Cranz or cube-root scaling [17]. The scale distance parameter Z is determined by the following equation based on the explosive equivalent TNT weight:

$$Z = R/W^{1/3} \quad (1)$$

Where R is the standoff distance from the blast source, and W is the equivalent TNT charge weight. Explosion induces significant pressures and suctions on different surfaces and points of a building, and the amount of this pressure can be measured by the scaled distance (Z). The distance between the detonation charge and the points on the building block (denoted as R_i , in Figure (2)) is calculated by equations 2-4.

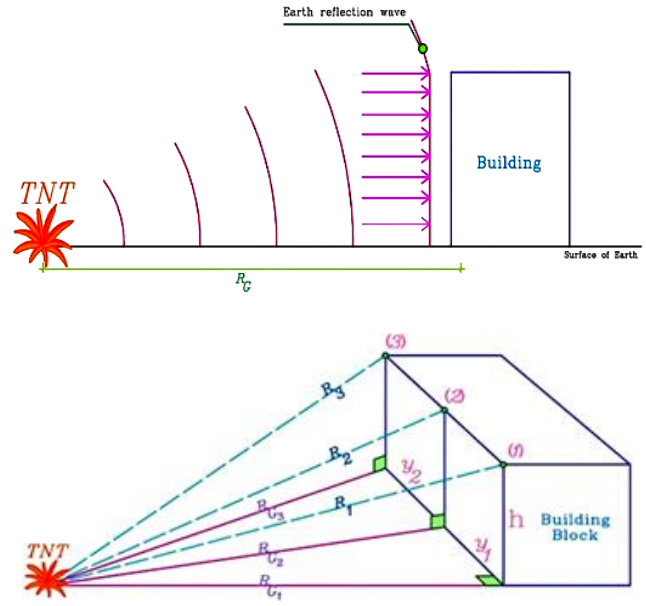


Fig. 2: Building geometry to calculate R_i

$$R_1 = (R_{G_1}^2 + h^2)^{1/2} \quad (2)$$

$$R_{G_2} = (R_{G_1}^2 + y_1^2)^{1/2} \rightarrow R_2 = (R_{G_2}^2 + h^2)^{1/2} \quad (3)$$

$$R_{G_3} = (R_{G_2}^2 + y_2^2)^{1/2} \rightarrow R_3 = (R_{G_3}^2 + h^2)^{1/2} \quad (4)$$

Various equations have been proposed by researchers to predict the blast parameters and peak overpressure resulting from the blast wave movement. Peak overpressure, P_{so} , was first formulated by Brode in 1955 as follows [18]:

$$P_{so} = \frac{6.7}{Z^3} + 1 \quad (P_{so} > 10 \text{ bar}) \quad (5)$$

$$P_{so} = \frac{0.975}{Z} + \frac{1.445}{Z^2} + \frac{5.85}{Z^3} - 0.019 \quad (0.1 < P_{so} < 10 \text{ bar}) \quad (6)$$

In which, Z is the scaled distance, W shows the equivalent weight of TNT, and R is the distance of blast point to the structure. Also, Henrych proposed an equation to measure the maximum blast overpressure in 1979 [19].

$$P_{so} = \frac{14.072}{Z} + \frac{5.54}{Z^2} + \frac{0.357}{Z^3} + \frac{0.00625}{Z^4} \quad (0.05 < Z < 0.3) \quad (7)$$

$$P_{so} = \frac{6.194}{Z} + \frac{0.326}{Z^2} + \frac{2.132}{Z^3} \quad (0.3 < Z < 0.1) \quad (8)$$

The positive time duration is presented by Equation (9), which is proposed by Lam et al. [20].

$$t_0 = W^{1/3} \times 10^{[-2.75 + 0.27 \log Z]} \quad (9)$$

Rankine [21] determined the explosive wavefront velocity U as follows:

$$U = a_0 \sqrt{\frac{6P_{so} + 7P_0}{7P_0}} \quad (10)$$

In which P_0 and a_0 stand for the ambient air pressure (which is usually 101 KPa) and the sound speed in the air (335 m/s), respectively.

The duration between the incident of explosion and the arrival of blast wave (t_A) is defined by Equation (11):

$$t_A = \frac{R_h}{U} \quad (11)$$

Coefficient C_r is determined by Equation (12) (Lam et al [20]):

$$C_r = 3 \sqrt[4]{\frac{P_s}{101}} \quad (12)$$

The reflected overpressure is calculated by Equation (13):

$$P_r = C_r \times P_{s0} \quad (13)$$

Finally, the time history of blast impact wave pressure is determined based on Friedlander's exponential-decaying equation as follows:

$$P = P_r \left(1 - \frac{t-t_A}{t_0}\right) e^{-\frac{\gamma(t-t_A)}{t_0}} \quad t > t_A \quad (14)$$

$$P = 0 \quad t < t_A$$

In the above equations, t_A and γ are the blast wave arrival time and the amplitude decay rate of blast pressure, respectively. t_0 is positive phase of blast duration of blast pressure:

$$\gamma = Z_h^2 - 3.72Z_h + 4.2 \quad (15)$$

Besides, the graphs to determine the blast parameters are presented by UFC 30-340-02 [22] and TM5-1300 [23].

In the present research, the verification of the numerical model is achieved through a comparison of the calculated numerical results with the ones presented by experiments. The empirical results, calculated by Brode and Henrych equations [18-19], are compared with the verified numerical results. In the next part of this paper, the sampled structures are excited by the numerical and empirical formulation of Brode pressure time histories to implement the non-linear dynamics of the tested structures against the blast wave.

2.3 Blast impact wave interaction with the building

Blast waves move at a speed which is more than sound speed and form a wavefront [22]. As a result of this waveform formation, the building is exposed to the blast pressure. It rises on the surface for a short moment and reaches its maximum due to the reflection of the waves of the building surfaces. The wavefront is reflected onto the lateral surface and refracts of the building and the corners (Figure (3)). This can lead to a decrease or an increase in the blast wave pressure. This process continues until all parts of the building are affected by the blast wave pressure.

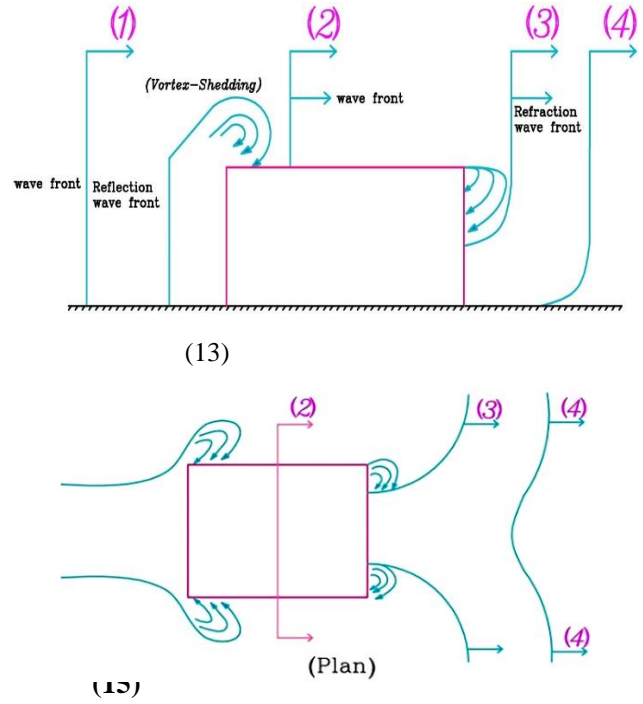


Fig. 3: Interaction of blast wave with the structure, blast- induced pressure is reflected in the side area and is refracted in the top area of the building. These effects are extended to the rare side of the building

To design and assess structures against explosion effects, we need to calculate the intensity of the loads resulting from the explosion exerted on the front, rare, sides, and roof surfaces of the building. To this aim, we need to consider the interactions between the blast impact waves and the building. When a building is affected by a blast wave, it is loaded by the excess pressure and suction forces resulting from the explosion. This interaction can be categorized into three different situations based on the building size:

- Interaction between the blast impact wave and a rectangular building with a limited size
- Interaction between the blast impact wave and a relatively small structure all sides of which are affected by the blast wave pressure at once.
- Interaction between the blast impact wave and a relatively large building, such as a tall building, in which the blast wave intensity varies significantly across the surfaces of the structure [24].

Validation and simulation of the blast load on one-story and ten-story buildings were assessed in this study. Therefore, all of the situations mentioned above were used to calculate the blast load.

2.4 Numerical simulation of blast wave propagation

2.4.1 Material models and state equations

The most accurate method, to determine the blast wave pressure-time history, is using computational fluid dynamics

(CFD) and hydrocode software. In this method, the explosive material and air are simulated, and the real blast wave pressure history on different points of the structure is calculated based on reflections off other surfaces of walls, roof, ground, and the interaction among them. The 3D Euler equations were applied for the computations complemented with the ideal gas equation of state for air and the JWL equation of state for TNT. History of numerical simulations and different methods of Eulerian, Lagrangian, and mixed meshing are presented by Zunaks [25-26]. Fundamentally, the equation of state shows thermodynamic equality that formulates the relationship between temperature, volume, and internal energy as a mathematical equation. Equation of state is presented as follows:

$$P = A \left(1 - \frac{\omega}{R_1 V}\right) e^{(-R_1 V)} + B \left(1 - \frac{\omega}{R_2 V}\right) e^{(-R_2 V)} + \frac{\omega e_0}{V} \quad (16)$$

Where P is hydrostatic pressure, $V=1/\rho$ stands for the specific volume, ρ stand for the density, e stands for the specific internal energy and A , B , R_1 , R_2 , ω are empirical constants. They have been evaluated using dynamic experiments. Their values are presented in Table 1 [27].

Table 1: Values of empirical constants in (27)

A (KPa)	B (Kpa)	R_1	R_2	E (kJ/m ³)	ω	ρ (Kg/m ³)
3.7377×10^8	3.7471×10^6	4.15	0.9	6×10^6	$\frac{0.3}{5}$	1630

The AUTODYN-3D hydrocode [28] is applied to solve the numerical equation of blast wave propagation. AUTODYN-3D is specifically designed to solve the non-linear dynamics of fluids, gases, and solids problems. This tool uses finite difference, finite volume, finite element, and smoothed-particle hydrodynamics methods to discretize and solve the problems. This type of software is known as a ‘hydrocode.’ The most crucial use of hydro codes, which are also known as wave propagation codes, is in the simulation of the blast wave in fluids and solids and simulation of non-linear dynamics problems such as impact, penetration, and explosion. This program can study the phenomena which are characterized as being highly time-dependent while both geometric and material nonlinearities are involved.

2.4.2 Simulation verification

Generally, the most significant part of the analysis using the numerical models is to verify the calculated results. To validate the modeling, numerical analysis, and the software, we need to make use of experimental findings in line with the study. In this regard, an experimental test was selected form reference [27]. Validation of the results is done by the following simulations:

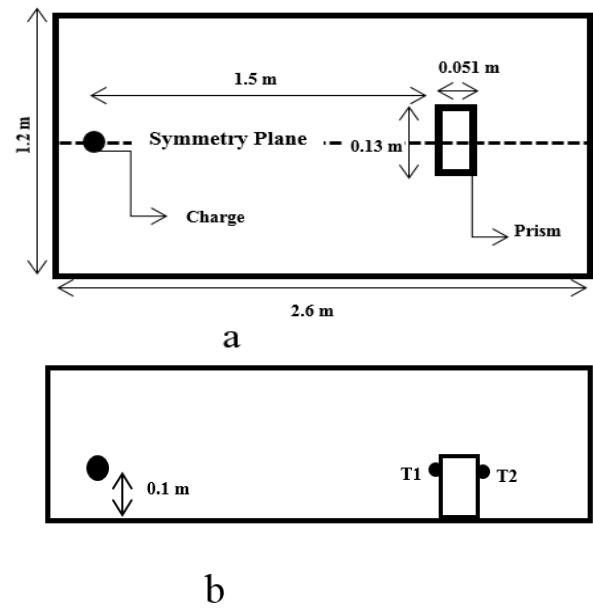


Fig. 4: Plan view (a), centrally cross-section (b)

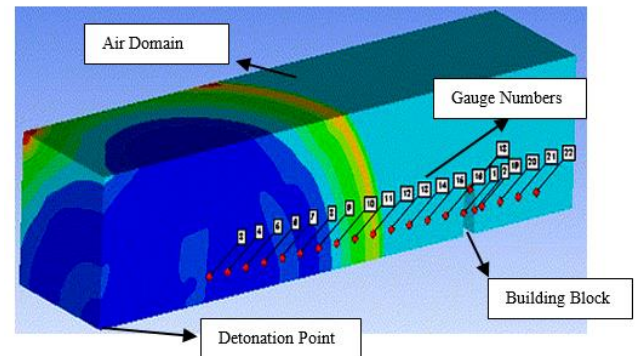


Fig. 5: Numerical simulation

Four different states of mesh size, with hexagonal cells of equal size, were selected, as presented in table 2

Table 2: Various mesh sizes

Grid #	Cell size in x-direction, cm	Cell size in y-direction, cm	Cell size in z-direction, cm
1	1	1	1
2	0.5	1	1
3	0.25	1	1
4	0.5	0.5	0.5
N_x	N_y	N_z	Total cell number
260	60	60	936000
520	60	60	1872000
1040	60	60	3744000
520	120	120	7488000

Figure 6, the calculated pressure-time history by numerical simulation in AUTODYN-3D, is compared with the findings of Fedorova et al. [27] and experimental results. Also, figure 7 compares the numerical outcomes of the maximum of the blast impact wave pressure relative to the ambient pressure as a function of scaled distance with empirical relations introduced by Brode and Henrych.

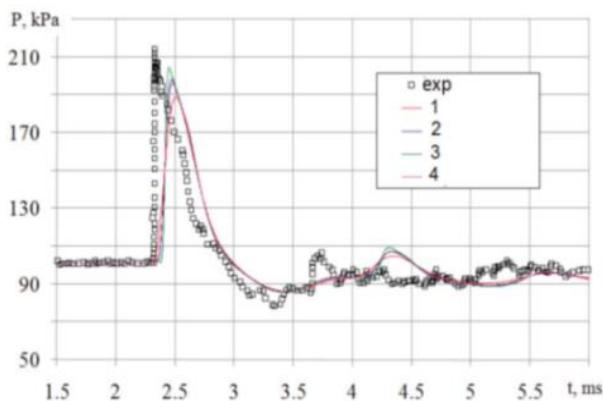
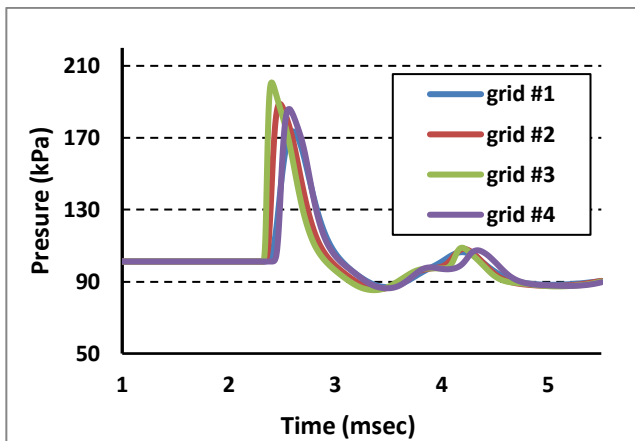


Fig.6: Numerical pressure-time history using AUTODYN and experimental results by Fedorova et al. of T1 gauge

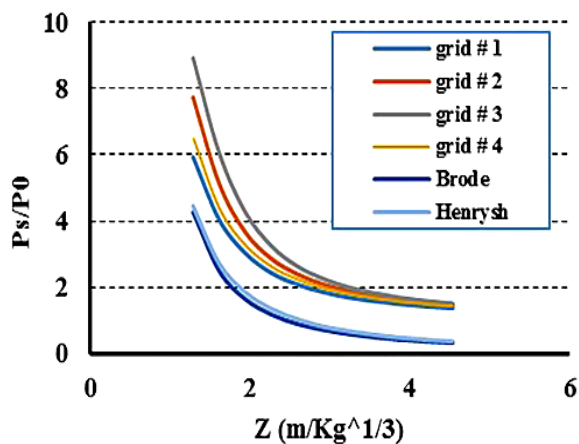


Fig. 7: Maximum of blast-induced pressure to ambient pressure ratio versus scaled distance

3. The sensitivity of response to the mesh size and the airflow surrounding the structure

3.1 Modeling method

In this paper, to study the sensitivity of blast-induced pressure to the building mesh sizes and air cubic dimension, a 3-D one-story building block is modeled in AUTODYN-3D. The dimensions of the building block are 14×14×4 meters (see figure 8). The block is meshed using hexagonal elements. The model volume consists of explosion material

(TNT), surrounding air, and the structure. Due to symmetry, only half of the domain was modeled. To study the effect of mesh sizes, eight mesh sizes are considered. They are five uniform mesh sizes (2.5, 5, 10, 15 and 30 cm) (see Figure 9). The pressure gauges are placed in longitudinal and transverse directions in the surrounding air and on the front, rear, side, and roof faces of the building block. To evaluate the effect of cube sizes of the surrounding airflow, various values of B_s , B_b , and B_{side} (defined in Figure 10) are considered, assuming the constant detonation distance. The explosion charge of 50 kg in 5 meters distance of the building block is assumed as the explosion scenario. The sensitivity analysis is implemented for the one-story building to achieve the suitable mesh and air cube sizes, which will be applicable for the other sampled structure (i.e., 10-story building) in this paper. The scaled distances for the case mentioned above are 1.3 to 2.3 $\text{m/kg}^{1/3}$ in the transverse direction and 0.7 to 1.38 $\text{m/kg}^{1/3}$ in the longitudinal direction. It is worth mentioning that the blast scenario with a scaled distance of 0.5 to 1.5 $\text{m/kg}^{1/3}$ will cause moderate damage to the structures.

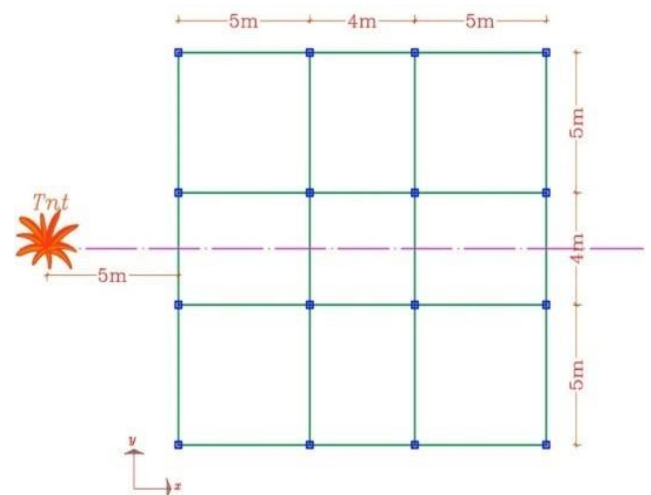
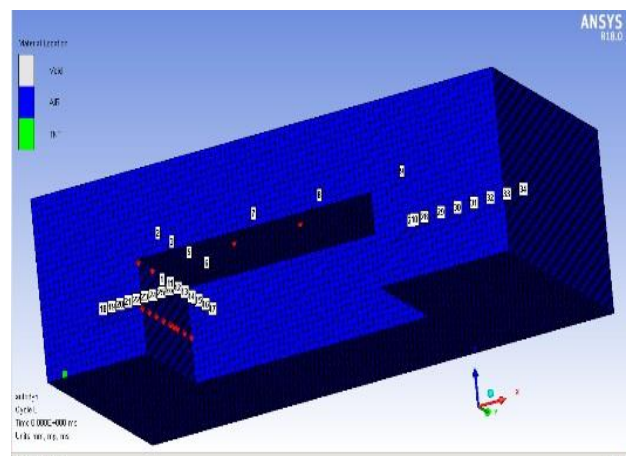


Fig. 8: Plan view of the studied building



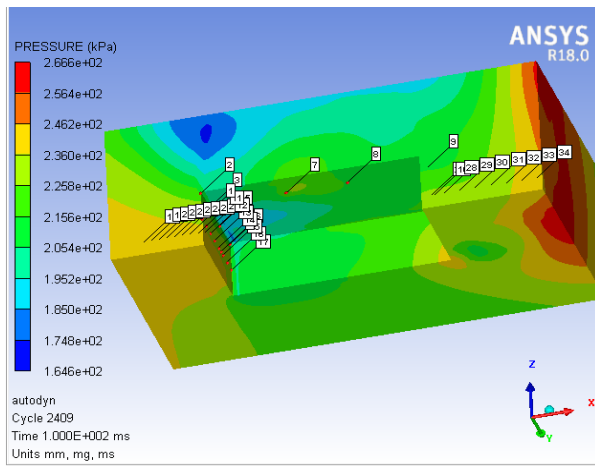


Fig. 9: Uniform meshing and pressure gauges' location

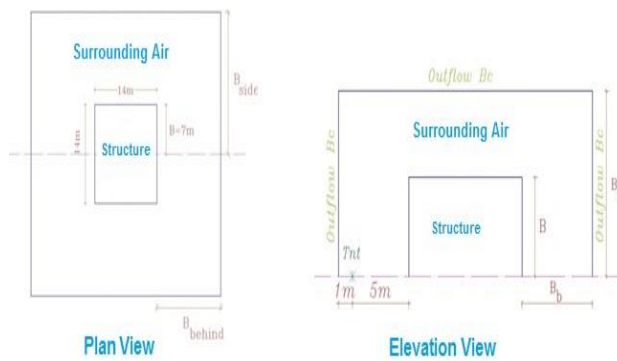


Fig. 10: Problem domain

The calculation domain, considering symmetry about the x-axis, was $8 \times 15 \times 28$ m, and numerical analyses were conducted using a server with 128 GB of RAM and two E5-2695 V4-2.1GHz CPUs. The numerical simulations, along with different mesh sizes, the number of elements, the total analysis time, and the various conditions of the air cube dimension, were chosen according to tables 3 and 4. For instance, to simulate 30 milliseconds with nearly 24 million 5 centimetres uniform mesh, 270 hours with a server with the specifications mentioned above was necessary. In the tables 3, N_x , N_y and N_z are number of elements in x, y and z directions, respectively. The modelling parameters in table 4 (B , B_s and B_b) are presented by Figure 10.

Table 3: Size and number of uniform meshing

Cell size in x-direction, cm	Cell size in y-direction, cm	Cell size in z-direction, cm	Total cell number	The time duration of analysis
2.5	5	5	x-axis symmetry 53.76e6	270 Hr.
			x, y-axis symmetry 17.8e6	93 Hr.
5	5	5	23 744 000	114 Hr.
10	10	10	2 968 000	20 Hr.
15	10	15	1310 880	38 minutes
30	20	30	165 295	15 minutes

Table 4: Various cases for structure surrounded air flow cubes

type	B_b	B_s	h_{air}
1	2B	B	2h
		2B	2.5h
		3B	3h
2	3B	B	2h
		2B	2.5h
		3B	3h

3.2 Numerical results

The numerical analysis results are shown in Figure 11. In Figure 16, P_s , P_r , and P_0 stand for the maximum overpressure, reflected pressure and ambient pressure, respectively. Besides, the empirical curves, based on Henry and Brode formulations, are compared with the numerically calculated results.

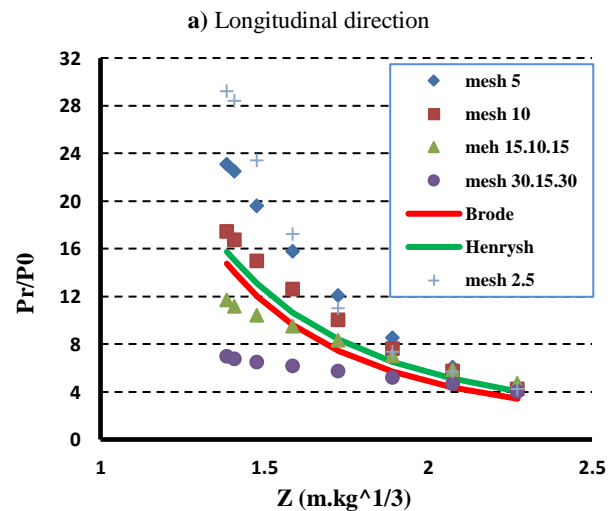
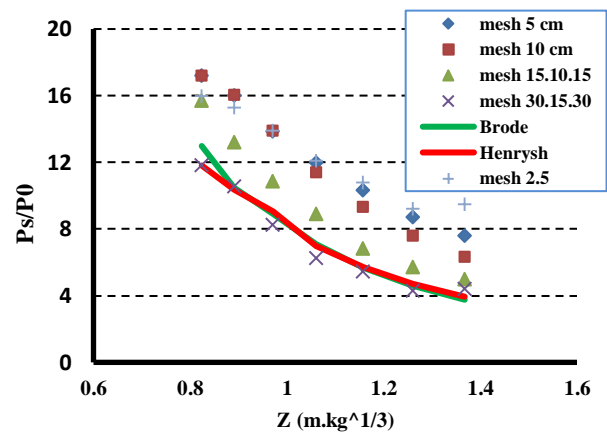


Fig. 11: Effect of mesh size on the maximum blast-induced pressure to air pressure ratio for various blast scaled distance

As can be seen from the above Figures, for various scaled distances of explosion scenarios, the accuracy of empirical equations in the near field is not satisfactory. Mesh size affects the maximum pressure, reflection, and refraction of the wave. Figure 12 shows the effect of mesh size on the

blast wave reflection of barometer number 24 at a one-meter distance from the building with $Z = 1.26 \text{ m/kg}^{1/3}$.

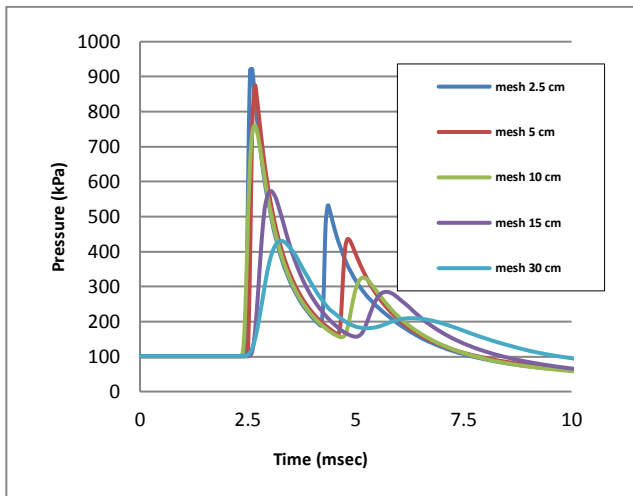


Fig. 12: Effect of meshing size on reflection and refraction of blast impact wave

Figures 13 and 14 demonstrate the pressure-time history of the rare and roof sides of the roof with changes in the dimensions of the airflow cube surrounding the building.

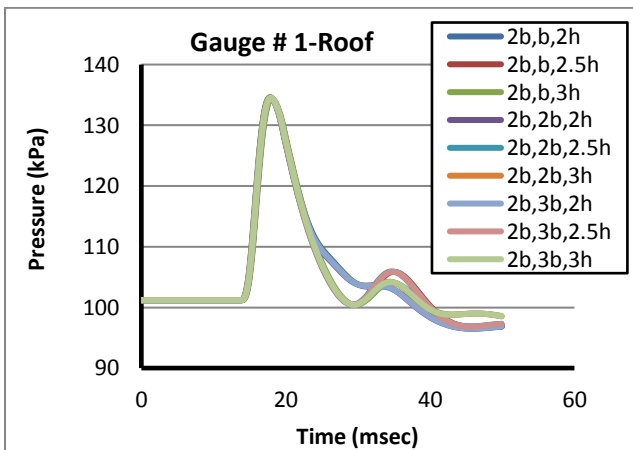
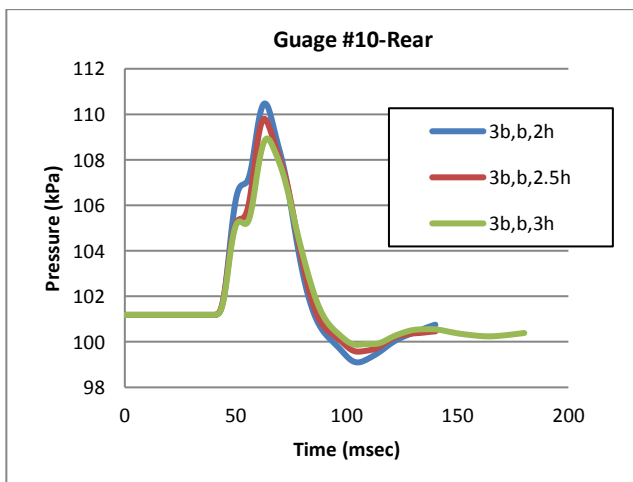
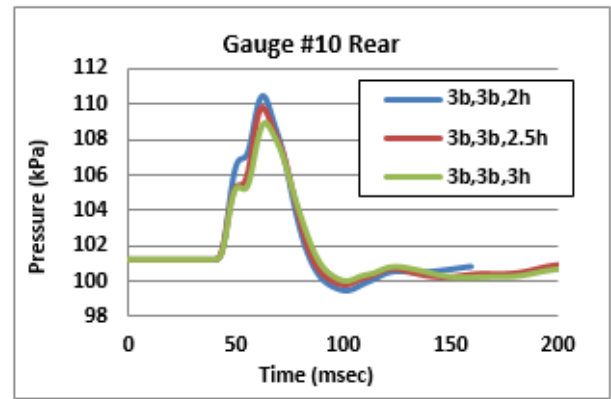


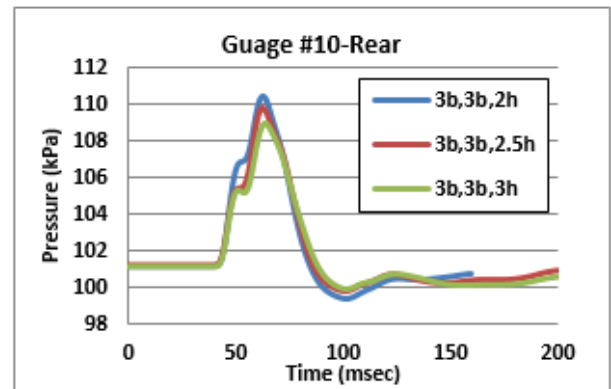
Fig. 13: Pressure-time history of the roof



14-a) Air cube dimensions variations ($b_b, h_{air}, b_s = 2b$)



b) Air cube dimensions variations ($b_b, b_s = 3b, h_{air}$)



c) Transverse direction $b_b, b_s = 2b, h_{air}$

Fig. 14: Effect of air cube dimension on Pressure time history for rear and roof of the building

4. Numerical Simulation of Realistic Blast Scenario Effects on the 10-Story building

After determining the appropriate mesh and air cube sizes for numerical simulation, the effects blast loading on the 10-story building is assessed modeling 3-dimensionally. The model is the one-story building in 4.1. The number of stories is increased to 10, and each story is 3.2 meters high. The explosion scenario includes placing 600 KG of TNT ten meters away from the building. This scenario is selected according to the UFC 3-340-02 regulation [22]. It considers the amount of explosives that can be transported by a vehicle [29]. Selected mid-range explosive charges are placed on the building to simulate terrorist attacks on buildings. Figure 15 represents the numerical simulation of the ten-story structure in AUTODYN-3D software along with the pressure gauge locations on the height of the side facing the explosion, the lateral sides, and the roof. For the sake of symmetry and to reduce the computational time, a quarter of the building is modeled along with the surrounding airflow cube. The structure is defined as an 'unused' rigid area [28] and acts as a rigid surface.

The computational domains were the volume of air with the initial parameters corresponding to the normal atmospheric

conditions in 2.4.1 section. In this method, the explosive material and air are simulated, and the real blast wave pressure history on different points of the structure is calculated based on reflections off other surfaces of walls, roof, ground, and the interaction among them. The 3D Euler equations were applied for the computations complemented with the ideal gas equation of state for air and the JWL equation of state for TNT.

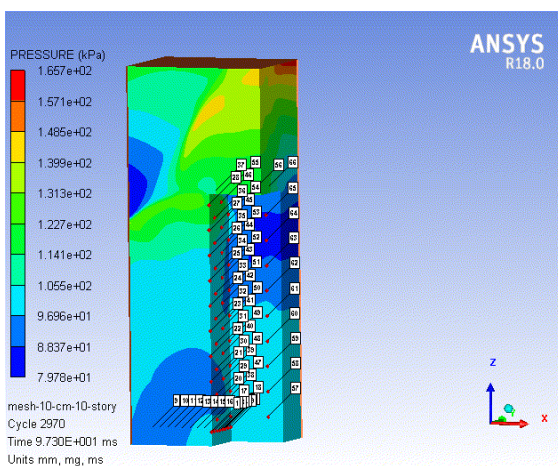
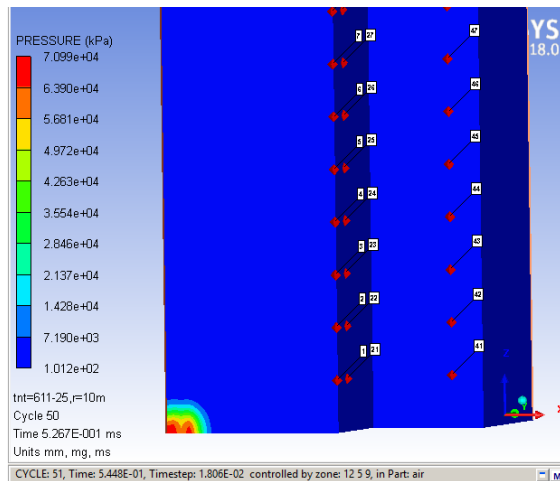


Fig. 15: 10-story model of the structure and the relevant surrounding airflow, pressure gauge at height

5. Performance Assessment of 1 and 10-Story Buildings

To assess the performance of structures against numerically simulated blast wave two sampled structures are considered. The sampled buildings are designed based on national seismic code (standard No. 2800), the buildings were modeled and designed in SAP2000 software using the LRFD method and according to AISC 360-10. The cross-sections of the designed beams and columns and specifications of the building materials of the numerical model for the 3D finite element model in OpenSees are stated in table 5. Afterwards, in order to assess the performance of the buildings in the explosion scenario, the structures were modeled in 3D using OpenSees finite element tool [30]. Afterwards, using non-

linear dynamics under the calculated blast loads using CFD and empirical loading from Brode's relation and according to the UFC regulation, the structures were analyzed. The nonlinear finite element model consists of fiber element using Steel02 material. (The Elasto-plastic material model considering the hardening effect was employed for steel). The pressure-time history of the blast resulting from the numerical simulation and Brode's empirical relation for the 3D finite element model in OpenSees is represented in figures 16-21.

Table 5: Numerical model properties

Type of model	Stories	Column section (cm)	Beam section (cm)	Structural properties:
3D frame (1 Story)	1	Box 45×45×2.5	PL 30×0.8×15×1	Story height=3.2 m Material properties: $F_y = 248 \times 10^6 \text{ N/m}^2$, $F_u = 400 \times 10^6 \text{ N/m}^2$ Mass density = 7698 kg/m ³ Poisson's ratio = 0.3 Modulus of elasticity = $2 \times 10^{11} \text{ N/m}^2$
3D frame (10 Story)	1-6 7-10	Box 70×70×3.5 Box 50×50×2	PL 30×1×15×1.5 IPE 300	

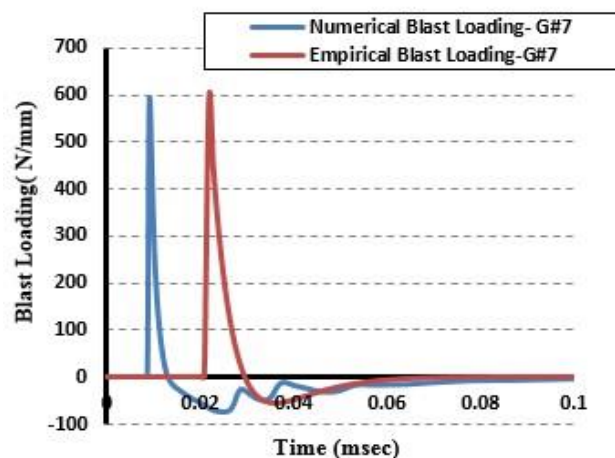


Fig. 16: Applied load per length of column (Gauge g7 at 1-story)

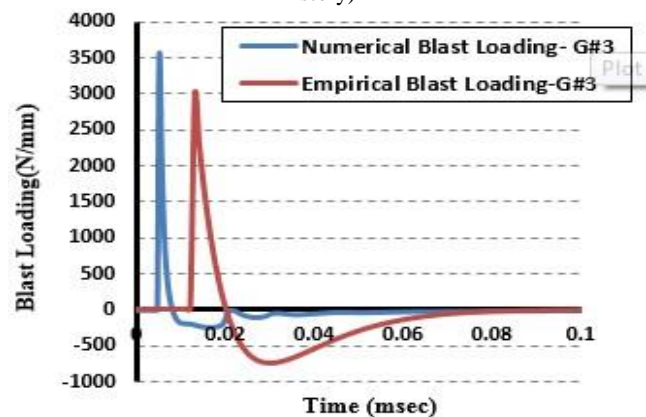


Fig. 17: Applied load per length of column (Gauge g3 at 1-story)

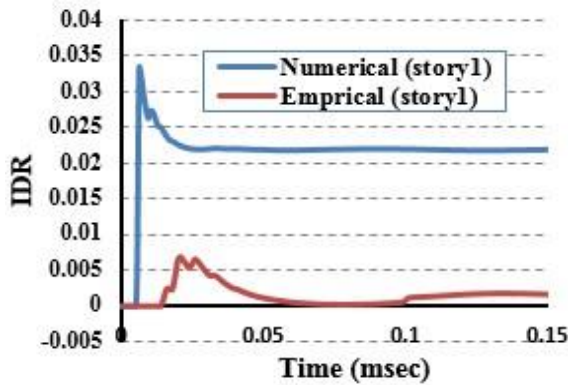


Fig. 18: Inter-Story drift for the 10-story building

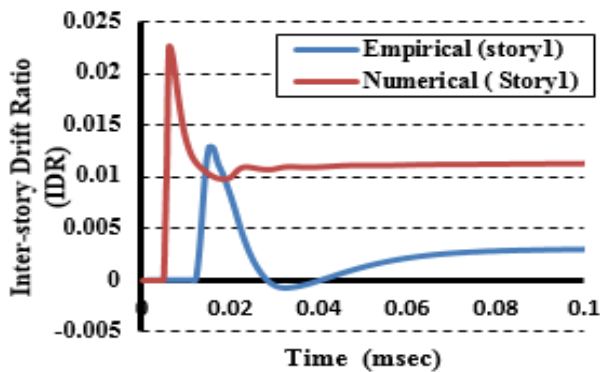


Fig. 19: Inter-Story drift for the 1-story building

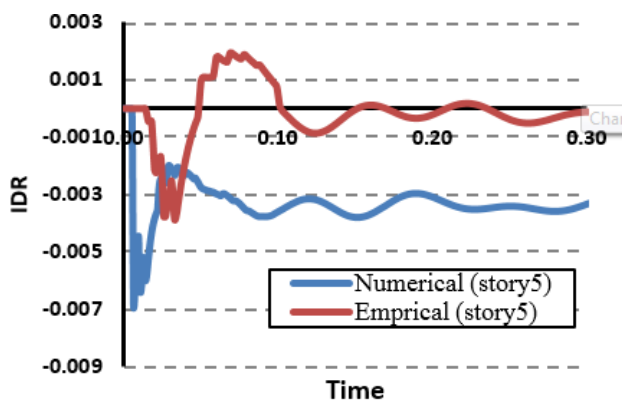


Fig. 20: Inter-Story drift for the 5-story building

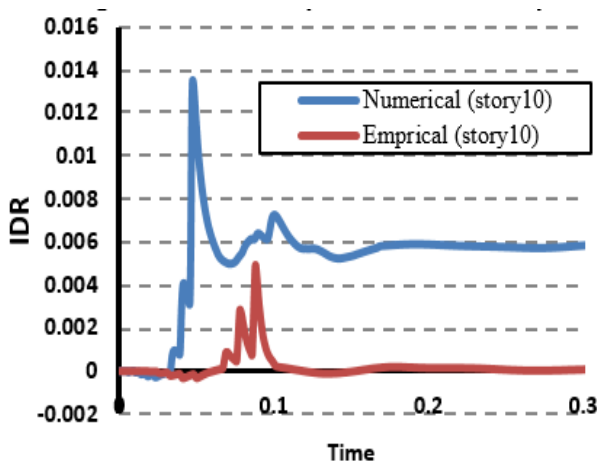


Fig. 21: Inter-Story drift for the 10-story building

6. Conclusion

In the present research, the effects of mesh size and dimension of air cube, flowing surrounding the structure, on the simulated blast shock wave affected the building structures, are assessed. Furthermore, the suitable mesh size is proposed according to the scaled distance and standoff distance. The sensitivity analysis is implemented for the one-story building to achieve the suitable mesh and air cube sizes, which will be applicable for the other sampled structure (i.e., 10-story building) in this paper. Finally, two seismically-designed tested structures of one, and ten stories are analyzed against achieved numerical blast waves. To evaluate the structural performance against blast loading, the structural analyses are performed against the numerical blast wave and empirical formulation of the blast wave based on UFC 3-320-02. The 3D model of the structure is implemented using OPENSEES. The nonlinear dynamic analysis results are calculated towards performance assessment based on FEMA-356 criteria, for which the peak inter-story drift ratio (MIDR) is the measure of structural performance.

Numerical simulation of the blast wave for various mesh sizes reveals that the difference between the numerical and experimental responses is increased when the scaled distance decreases. Furthermore, the more scaled distance is, the less will be the relevant sensitivity to the mesh size.

In transverse direction (perpendicular to the longitudinal direction of wave propagation), as the scaled distance increases, the dependability of maximum pressure on mesh size decreases. Also, there is good conformity between numerical results and empirical relations in the above-scaled distances. As we saw in the validation model, the difference between numerical results increases when the scaled distance decreases. This result shows that the accuracy of the empirical relations for small-scaled distance is not guaranteed and that they are suitable for the mid and far scaled distances. In the longitudinal direction, as the scaled distance increases, the dependability of the overpressure on mesh size increases. Furthermore, the difference between numerical and empirical results increases.

Mesh size affects the simulated results of reflection and refraction of the blast wave. While the mesh size increases, the reflection effect of the blast wave in the numerical model is decreased. This reduction is in such a way that for the mesh size larger than 30 cm, the reflection effect vanishes. Usually, the 10 centimeters mesh is a suitable mesh for blast wave propagation in 3D buildings, especially in urban areas. As expected, the numerical results reveal that in the longitudinal direction of wave propagation, the smaller the mesh is, the better the response will become. The time of arrival blast wave impact does not depend on mesh size. However, since limited blast scenario is assumed to achieve

these conclusions, it is declared that the mesh sizes mentioned above are not necessarily unique.

Numerical methods provide a better estimate compared with empirical methods because essential effects such as blast wave reflection, Mach effect, blast wave suction, and rarefaction are readily involved in the computational fluid dynamics routines. In contrast, while these significant effects are not included in empirical relations, which could lead to crucial underestimation of the peak values in the blast scenarios with far scaled distances.

The following findings resulted from analyzing the sensitivity of selecting the dimensions of the airflow cube surrounding the building in the simulation:

If the distance between the explosive charge and the structure is constant, it is expected that making changes in the airflow cube dimensions (width, height, and length of the back of the structure) will not change the overpressure within the longitudinal and transverse limits, which is logical. Only, mesh size affects the overpressure.

The pressure-time graphs of the gauges behind and on the roof of the building are entirely in accordance when the airflow cube dimensions (length and width) change behind the building. The overpressure changes slightly if the airflow cubes height changes (h, 2.5h, 3h) in such a way that as the height increases, the overpressure decreases. Consequently, it is better to use airflow cube dimensions that have the smallest analysis volume.

As seen in figures, pressure-time graphs of lateral sides show a considerable suction compared with the surface facing the explosion. Also, the pressure graphs show the refraction and reflection of blast waves on lateral sides and the roof. The effects of the blast on the lateral and back sides and roof are insignificant compared with the effects on the side facing the explosion, and the latter is 5-6 times greater than the former. The structures' performance against numerical explosive loads exceeds the life safety (LS) level while being lower than the immediate occupation (IO) level for empirical blast load. Regarding the structural performance, the achieved results demonstrate that the performance of the assumed structure is not affected by the side, rear, and roof blast pressure. Somewhat it is affected by the blast pressure on the front side of the structure.

Conflicts of interest

The authors declare that there is no conflict of interest.

References

- [1] Laminou, L. M., Liu, Z., & Chen, X. H. (2019). Extreme events design and mitigation methods: A review. *Civil Engineering Journal*, 5(6), 1424-1439.
- [2] Krauthammer, T., & Otani, R. K. (1997). Mesh, gravity and load effects on finite element simulations of blast loaded reinforced concrete structures. *Computers & structures*, 63(6), 1113-1120.
- [3] Luccioni, B., Ambrosini, D., & Danesi, R. (2006). Blast load assessment using hydrocodes. *Engineering Structures*, 28(12), 1736-1744.
- [4] Chapman, T. C., Rose, T. A., & Smith, P. D. (1995). Blast wave simulation using AUTODYN2D: A parametric study. *International Journal of Impact Engineering*, 16(5-6), 777-787.
- [5] Dharaneepathy, M. V., Rao, M. K., & Santhakumar, A. R. (1995). Critical distance for blast-resistant design. *Computers & structures*, 54(4), 587-595.
- [6] Ghanbari, H. Salajegheh, E, and Salajegheh, J. (2018). Assessment of numerical simulation of blast wave propagation on building structures. *8th National Conference on Earthquake and Structures*.
- [7] Ghanbari, H., Salajegheh, E., Khojastehfar, E, and Salajegheh, J. (2019). Performance assessment of seismically-designed steel moment-resisting frames against numerical simulated of the blast wave. *8th International Conference on Seismology & Earthquake Engineering*.
- [8] Wenjiao, Z. (2018). Numerical simulation of cracked reinforced concrete slabs subjected to blast loading. *Civil Engineering Journal*, 4(2), 320-333.
- [9] Tavakoli, R., Kamgar, R., & Rahgozar, R. (2018). The best location of belt truss system in tall buildings using multiple criteria subjected to blast loading. *Civil Engineering Journal*, 4(6), 1338-1353.
- [10] Bevins, T. L., Armstrong, B. J., Baylot, J. T., & Rickman, D. D. (2003, June). Multiple building simulations and effect of berms behind blast barrier walls. In *2003 User Group Conference. Proceedings* (pp. 250-256). IEEE.
- [11] Sugiyama, Y., Homae, T., Wakabayashi, K., Matsumura, T., & Nakayama, Y. (2014). Numerical simulations on the attenuation effect of a barrier material on a blast wave. *Journal of Loss Prevention in the Process Industries*, 32, 135-143.
- [12] Flood, I., Bewick, B. T., & Rauch, E. (2012). Rapid Simulation of Blast Wave Propagation in Built Environments Using Coarse-Grain Simulation. *International Journal of Protective Structures*, 3(4), 431-448.
- [13] Kinney, G. F., & Graham, K. J. (2013). *Explosive shocks in air*. Springer Science & Business Media.
- [14] Draganić, H., & Sigmund, V. (2012). *Blast loading on structures*. Tehnički vjesnik, 19(3), 643-652.
- [15] Chipley, Michael. (2003). *Reference Manual to Mitigate Potential Terrorist Attacks Against Buildings*. Providing Protection to People and Building. Federal Emergency Management Agency, FEMA 426, Chapter 4, 1-20.
- [16] Hinman, E. (2003). Primer for design of commercial buildings to mitigate terrorist attacks. *Risk management series FEMA*. Federal Emergency Management Agency, Washington, DC.
- [17] Bangash, M. Y. H., & Bangash, T. (2005). *Explosion-resistant buildings: design, analysis, and case studies*. Springer Science & Business Media.

[18] Brode, H. L. (1955). Numerical solutions of spherical blast waves. *Journal of Applied physics*, 26(6), 766-775.

[19] Henrych, J., & Abrahamson, G. R. (1980). The dynamics of explosion and its use. *Journal of Applied Mechanics*, 47(1), 218. [20] Lam, N. T. K., Mendis, P., & Ngo, T. (2004). Response spectrum solutions for blast loading. *Electronic Journal of Structural Engineering*, 4, 28-44.

[21] Rankine, W. J. M. (1998). XV. On the thermodynamic theory of waves of finite longitudinal disturbance. *Philosophical Transactions of the Royal Society of London*, (160), 277-288.

[22] Acosta, P. F. (2011). Overview of UFC 3-340-02 structures to resist the effects of accidental explosions. In *Structures Congress 2011* (pp. 1454-1469).

[23] Army Technical Manual 5-1300/NAVFAC P-397/AFR 88-22, US Department of the Army. (1990). *Design of structures to resist the effects of accidental explosions*.

[24] Kulkarni, A. V., & Sambireddy, G. (2014). Analysis of blast loading effect on high-rise buildings. *Civil and Environmental Research*, 6(10).

[25] Zukas, J. A. (1980). *Impact dynamics: theory and experiment*. ARMY BALLISTIC RESEARCH LAB ABERDEEN PROVING GROUND MD.

[26] Zukas, Jonas A., ed. (1990). *High velocity impact dynamics*. Wiley-Interscience.

[27] Fedorova, N. N., Valger, S. A., & Fedorov, A. V. (2016, October). Simulation of blast action on civil structures using Ansys AUTODYN. In *AIP Conference Proceedings* (Vol. 1770, No. 1, p. 020016). AIP Publishing LLC.

[28] AUTODYN user's manual-revision 4.3.(2003). Century Dynamics Inc.

[29] Chipley, M., Lyon, W., Smilowitz, R., Williams, P., Arnold, C., Blewett, W., ... & Krimgold, F. (2012). Primer to Design Safe School Projects in Case of Terrorist Attacks and School Shootings. Buildings and Infrastructure Protection Series. FEMA-428/BIPS-07/January 2012. Edition 2. *US Department of Homeland Security*.

[30] McKenna, F. (2011). OpenSees: a framework for earthquake engineering simulation. *Computing in Science & Engineering*, 13(4), 58-66.

[31] FEMA 356, F. E. (2000). Prestandard and commentary for the seismic rehabilitation of buildings. *FEMA Publication No.*, 356.

a_0	(which is usually 101 KPa)
t_A	Sound speed in the air (335 m/s)
	Duration between the incident of explosion and the arrival of blast wave
C_r	Reflected overpressure coefficient
P_r	Reflected overpressure
γ	Amplitude decay rate
P	Hydrostatic pressure
V	Specific volume
ρ	Density
e	Specific internal energy
$A, B, R1, R2, \omega$	Empirical constants



© 2023 by the authors. This article is an open-access article distributed under the terms and conditions of the Creative Commons Attribution (CC-BY)

List of notations

Symbol	Descriptions
R	Standoff distance
W	Equivalent TNT charge weight
Z	Scaled distance
P_{so}	Peak overpressure
t_0	Positive time duration
U	Wavefront velocity
P_0	Ambient air pressure